2024 European Control Conference (ECC)
June 25-28, 2024. Stockholm, Sweden

Dissipativity analysis for economic nonlinear MPC of district heating networks

Max Sibeijn[1] Saeed Ahmed[2] Mohammad Khosravi[1] Tamas Keviczky[1]

Abstract— **The inherently nonlinear, large-scale, and time-varying nature of district heating systems pose significant challenges from a control perspective. In this paper, we address these challenges by applying an economic MPC. Economic MPC is a dynamic real-time optimization method, enabling both optimal planning and stability of the closed-loop system. Our strategy constitutes several steps. First, we introduce a discrete-time modular framework for the district heating system, establishing its strict dissipativity with respect to a desired, potentially time-varying, equilibrium. We identify a set of meaningful objective functions for the district heating systems, preserving this property. Second, we show how strict dissipativity implies the turnpike property, which, in turn, guarantees approximate optimality, practical stability, and recursive feasibility for the EMPC closed-loop. Finally, we provide numerical simulations to demonstrate the effectiveness of our work.**

I. INTRODUCTION

The global energy landscape is undergoing a significant evolution, marked by the transition towards sustainable energy resources and the pressing need to reduce CO_2 emissions. In this regard, the integration of district heating systems (DHS) into the energy sector plays a crucial role because heating and cooling has approximately 50% contribution to the total energy demand within Europe [1]. One considerable challenge is the scheduling and control of DHS due to their large scale and due to inconsistent generation from renewable sources. However, the potential flexibility of DHS provides significant opportunities for its improvement with respect to the older generation systems. Achieving these improvements will require more advanced models, forecasts, and real-time optimal operational strategies.

Real-time optimal control for DHS has been studied in, for instance, [2], [3], where an MPC was designed using linearized thermal models, and in [4], where an alternative approach was pursued to deal with pressure drop in the network for fixed temperature supply and return dynamics. Recently, nonlinear optimization has found its way into the DHS control literature in two ways: *i)* by estimating the time delay in pipes [5], and *ii)* by discretizing the partial differential equations (PDEs) governing heat transport dynamics for optimal control [6], instantaneous (optimal) control [7], and adaptive (optimal) control [8]. Moreover, a nonlinear MPC for DHS was introduced in [9], however, closed-loop properties were not addressed.

Formerly, optimization and control of applications similar to DHS, such as the process industry, have been combined through a hierarchical two-step approach [10]. In this approach, the top level consists of a real-time optimization that computes optimal setpoints for the system in equilibrium, which are then fed to a low level stabilizing model predictive controller to regulate the system. Nonetheless, shortcomings of this approach arise, in particular, when slow dynamics drive the system, potentially leading to conservative decisions or infeasible setpoints caused by model inconsistencies [11]. On the other hand, benefits of a synthesized approach, called economic model predictive control (EMPC), include faster response to disturbances, no over-regulation, and exact constraint implementation (no safety margins); see [12].

EMPC is a generalization of stabilizing MPC, where the cost function is not necessarily a penalization of the distance to a specified equilibrium, but can encompass a broader range of objectives, such as energy minimization [13]. Nonetheless, closed-loop performance of EMPC does not inherently share the same guarantees as stabilizing MPC. Furthermore, for nonlinear or time-varying systems, it is often difficult to find suitable terminal conditions that ensure stability and recursive feasibility of the closed-loop [14]. Therefore, we require that the EMPC finds the optimal trajectory by itself. A key property for optimal control problems that ensures that the EMPC closed-loop solution remains close to the optimal trajectory is called the *turnpike property*. Evidence for the existence of this property can often be obtained empirically through simulation, however, there has been a substantial development in the literature indicating that the turnpike property can be implied from another property, called strict dissipativity; see [13], [14], [15], [16], [17], and [18].

For physical systems, strict dissipativity may be interpreted as the dissipation of energy to the environment. However, in the context of optimal control, even for the thermodynamic systems considered in this work, it does not have to serve this interpretation [15]. Particularly, this is because strict dissipativity is respective to a specific cost function and equilibrium, and this equilibrium does not need to be the one where the total energy stored is equal to zero. Generally, verification of strict dissipativity is not an easy task. It demands the existence of a storage function such that the dissipation inequality is satisfied at all times, which is difficult to check analytically in general. Therefore, a numerical approach was developed to verify strict dissipativity for continuous-time optimal control problems in [18] and for

[1]Delft Center for Systems and Control, Delft University of Technology, 2628 CN Delft, The Netherlands {m.w.sibeijn, mohammad.khosravi, t.keviczky}@tudelft.nl

[2]Jan C. Willems Center for Systems and Control, ENTEG, Faculty of Science and Engineering, University of Groningen, 9747 AG Groningen, The Netherlands s.ahmed@rug.nl

discrete-time problems in [19] and [20].

In this paper, we present a modeling framework for a DHS, demonstrating, both analytically and numerically, its strict dissipativity for a range of cost functions. Subsequently, we exploit this dissipativity to establish the turnpike property, which, in turn, implies approximate optimality, practical stability, and recursive feasibility for the closed-loop. To the best of our knowledge, this type of dissipativity analysis for EMPC has not been studied in the context of DHS. In the simulations section, we show empirical evidence for the turnpike property and demonstrate the performance of the EMPC.

The paper is structured as follows. In Section II, we introduce the model of a thermal node and how they can be interconnected to form two main types of thermal networks representing a DHS. In Section III, we provide the results on strict dissipativity of the thermal networks. In Section IV, we summarize implications this property has for EMPC, and finally, in Section V, we demonstrate the performance of the EMPC algorithm.

II. MATHEMATICAL MODEL

A. Modeling approach and assumptions

We consider a DHS to be a network of thermal components (pipe segments, heat exchangers, buffers, etc.), where we define this network on a connected directed graph $\mathcal{G} = (\mathcal{N}, \mathcal{E})$ with a set of nodes $\mathcal{N} = \{1, \dots, n\}$ connected by edges $\mathcal{E} = \{1, \dots, e\}$. A node, which we will refer to as a *thermal node* (TN) hereafter, represents a finite constant volume of water with a certain temperature. A thermal node interacts with other connected nodes, but also with its direct surroundings (see Fig 1). On the other hand, an edge defines which nodes interact with each other. Therefore, an edge has zero volume, but does have a temperature and velocity associated with it.

We model the thermal dynamics of a node through an approximation of the 1-dimensional compressible Euler equations for cylindrical pipes [7], [8]:

$$\frac{\partial \rho}{\partial t} + \frac{\partial (\rho v)}{\partial x} = 0, \tag{1a}$$

$$\frac{\partial (\rho v)}{\partial t} + \frac{\partial (\rho v^2)}{\partial x} + \frac{\partial p}{\partial x} + \rho g \hat{z} + K \frac{\rho}{2d} |v| v = 0, \tag{1b}$$

$$\frac{\partial T}{\partial t} + v \frac{\partial T}{\partial x} + \frac{p}{\rho c_p} \frac{\partial v}{\partial x} - \frac{K}{2 c_p d} |v| v^2 + \frac{4U}{\rho c_p d} (T - T_a) = 0, \tag{1c}$$

that describe the temporal and spatial evolution of three central variables; *temperature* $T(t,x)$ [K], the *flow velocity* $v(t,x)$ [m s^{-1}], and *pressure* $p(t,x)$ [Pa] of water. The other parameters are the density of water ρ [kg m^{-3}], gravity g [m s^{-2}], slope of pipe $\hat{z}$ [-], friction coefficient K [-], diameter of pipe d [m], heat transfer coefficient U [J m^{-2}K^{-1}], specific heat capacity of water c_p [J kg^{-1}K^{-1}], and ambient temperature T_a [K]. Let $q = Av$ (A being cross-section) denote the volume flow of water through a node. For simplicity, we assume that the mass flow q satisfies $q_{\max} \geq q \geq q_{\min} > 0$.

Subsequently, we introduce a set of assumptions that serve to derive a suitable model for optimization and control of the DHS.

Assumption 1: The water inside a thermal node is assumed to be incompressible, i.e., $\frac{\partial v}{\partial x} = 0$. Furthermore, the density of the water inside a thermal node is assumed to be constant, i.e., $\frac{\partial \rho}{\partial t} = 0$.

Assumption 1 is a fairly standard assumption in the literature; see e.g., [7] and [8]. Naturally, $\frac{\partial \rho}{\partial x} = 0$ follows from application of Assumption 1 to (1a).

Assumption 2: Heat losses from friction are very small compared to other terms in (1c), therefore, we assume $\frac{K}{2c_p d} |v| v^2 = 0$ as in [8].

Assumption 3: We neglect dynamics on the flow rate, i.e., $\frac{\partial v}{\partial t} = 0$, because of the significant separation in time scales between thermal and hydraulic dynamics, and because the frictional term in (1b) dominates the inertial term [6].

Finally, we are left with the following simplified stationary incompressible 1-dimensional Euler equations:

$$\frac{\partial p}{\partial x} + \rho g \hat{z} + K \frac{\rho}{2d} |v| v = 0, \tag{2a}$$

$$\frac{\partial T}{\partial t} + v \frac{\partial T}{\partial x} + \frac{4U}{\rho c_p d} (T - T_a) = 0. \tag{2b}$$

Consequently, equation (2a) does not depend on time and can be written as a nonconvex constraint, i.e. $g(v,p) = 0$. In what follows, we will not consider this constraint as we assume it can always be satisfied retrospectively, as long as the velocity is properly bounded. As a result, we are left with equation (2b). Before we introduce the model of a node, we require an additional assumption.

Assumption 4: The operational temperature in the network is always greater than or equal to the (maximum) ambient temperature.

This assumption is required to maintain nonnegativity of the states within the system, this is a technically motivated assumption but practically reasonable. In practice, even the lowest return temperature of a DHS typically exceeds the ambient temperature by some margin.

B. Thermal node model

A final step in defining a node model consists of a spatial discretization of (2b) according to an upwind scheme. This enables a spatially discrete formulation of finite volume cells in the network. Consequently, the dynamics of a thermal node $i \in \mathcal{N}$, can be described by the following scalar continuous-time ordinary differential equation (ODE):

$$\begin{aligned} V_i \dot{T}_i &= -q_i (T_i - T_{-i}) - \alpha_i (T_i - T_a) + h_i \\ y_i &= q_i T_i, \end{aligned} \tag{3}$$

where V_i denotes the node volume, $q_{\max} \geq q_i \geq q_{\min} > 0$ denotes mass flow of water, T_i denotes temperature of water in the node, T_{-i} is the temperature of the inflow into the node, and $\alpha_i = 4U_i / \rho c_p d_i$ is the heat loss coefficient. Additionally, if node i represents a heat exchanger, then the transfer of heat from one side to the other is defined by h_i; see [21].

A simple state transformation $x_i = T_i - T_a$, assuming w.l.g. that the ambient temperature is equal for all nodes, will let us write the dynamics as

$$\begin{aligned} V_i \dot{x}_i &= -(q_i + \alpha_i)x_i + u_i + h_i \\ y_i &= q_i x_i, \end{aligned} \tag{4}$$

which is graphically depicted in Fig 1, where $u_i = q_i x_{-i}$.

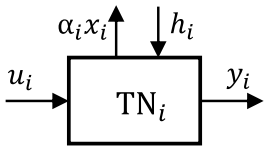

Fig. 1. A thermal node

C. Interconnection of thermal nodes

DHS are large-scale systems consisting of the interconnection of pipes, heat exchangers, buffers, etc. All of these components can be modeled using the previously defined thermal node model (4). In general, the physical connection between these components is by means of pipelines. Through these pipelines, water is transported from producer to consumer. Here, we introduce two types of network topologies that represent a DHS.

Definition 1 (Closed thermal network): A closed thermal network is a collection of thermal nodes $\mathcal{N}$ for which $\mathcal{G}$ is strongly connected. See Fig 2 for an example of a closed thermal network.

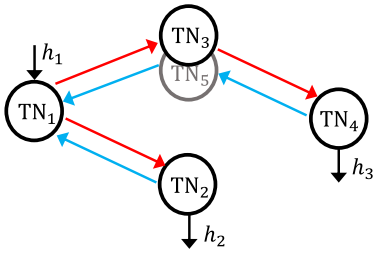

Fig. 2. A closed thermal network

Definition 2 (Open thermal network): An open thermal network is a collection of thermal nodes $\mathcal{N}$ such that $\mathcal{G}$ is weakly connected. Additionally, to ensure mass conservation, all source nodes have an external input acting on them (and all sink nodes have an output flow associated to them). See Fig 3 for an example of an open thermal network.

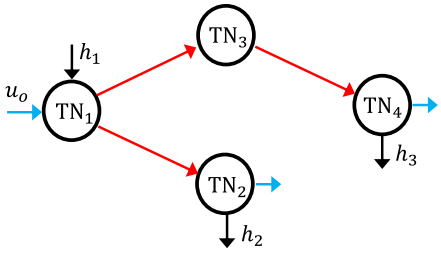

Fig. 3. An open thermal network

In addition, we require a rule for the mixing of multiple flows. To this end, we define two sets $\mathcal{E}_{-i}$ and $\mathcal{E}_{+i}$ for the incoming and outgoing edges of node i, respectively. The temperature of the inflow x_{-i} is determined by taking a weighted average of the temperatures of all edges directed towards node i (i.e., x_j for $j \in \mathcal{E}_{-i}$), where the weights are equal to the mass flows associated to each edge. Subsequently, based on [7], we define, for $i \in \mathcal{N}$,

$$x_j = x_i, \quad j \in \mathcal{E}_{+i}, \tag{5}$$

and

$$x_{-i} = \frac{\sum_{j\in\mathcal{E}_{-i}} q_j x_j}{\sum_{j\in\mathcal{E}_{-i}} q_j} = \frac{1}{q_i} \sum_{j\in\mathcal{E}_{-i}} q_j x_j, \tag{6}$$

where the last step follows from conservation of mass, which states that for a node $i \in \mathcal{N}$,

$$\sum_{j\in\mathcal{E}_{-i}} q_j = q_i = \sum_{j\in\mathcal{E}_{+i}} q_j. \tag{7}$$

In turn, conservation of mass is a result of Assumption 1.

Now, the interconnection between nodes is physically defined by the transfer of energy between them, hence, the coupling of these nodes can be realized by a static matrix that describes how the input energy u_i to TN_i depends on y_j as follows [22]:

$$u = M_{\mathcal{G}}(q) y, \tag{8}$$

where $u = \mathrm{col}(u_i)_{i\in\mathcal{N}}$, $y = \mathrm{col}(y_i)_{i\in\mathcal{N}}$, $q = \mathrm{col}(q_i)_{i\in\mathcal{N}}$, and $M_{\mathcal{G}}(q)$ is the transpose of the weighted adjacency matrix of $\mathcal{G}$ with each weight being q_j/q_i for $j \in \mathcal{E}_{-i}$.

Remark 1: In a closed network, (8) is equivalent to conservation of energy, meaning that $M_{\mathcal{G}}(q)\mathbf{1} = \mathbf{1}$. As a result, if we define the closed thermal network through this interconnection, energy conservation will be guaranteed. For example, in Fig 2, we have

$$M^c_{\mathcal{G}}(q) = \begin{bmatrix} 0 & \frac{q_2}{q_1} & 0 & 0 & \frac{q_5}{q_1} \\ 1 & 0 & 0 & 0 & 0 \\ 1 & 0 & 0 & 0 & 0 \\ 0 & 0 & 1 & 0 & 0 \\ 0 & 0 & 0 & 1 & 0 \end{bmatrix}.$$

On the contrary, for the open network in Fig 3, we get

$$M^o_{\mathcal{G}} = \begin{bmatrix} 0 & 0 & 0 & 0 \\ 1 & 0 & 0 & 0 \\ 1 & 0 & 0 & 0 \\ 0 & 0 & 1 & 0 \end{bmatrix}.$$

D. State-space representation of the DHS interconnection

We define the system in state-space form by substituting (8) into the system of equations that arises when the scalar equations in (4) are extended to a vector incorporating all x_i for $i \in \mathcal{N}$, for the two previously introduced thermal networks:

1) A closed thermal network:

$$\begin{aligned} V\dot{x} &= A_c(q)x + Bh, \\ z &= Cx, \end{aligned} \tag{9}$$

2) An open thermal network:

$$\begin{aligned} V\dot{x} &= A_o(q)x + B_o u_o + Bh, \\ z &= Cx, \end{aligned} \tag{10}$$

where $x = \text{col}(x_i)_{i\in\mathcal{N}}$, $V = \text{diag}(V_i)_{i\in\mathcal{N}}$, $h = \text{col}(h_i)_{i\in\mathcal{W}}$ with $\mathcal{W} = \{i : h_i \neq 0\}$, $u_o = q_o x_o \in \mathbb{R}^{n_o}$ with n_o the number of open connections (i.e., blue inflows in Fig 3), and

$$A_{c/o}(q) = -Q(I - M_{\mathcal{G}}^{c/o}(q)) - D_\alpha,$$

with $Q = \text{diag}(q)$ and $D_\alpha = \text{diag}(\alpha_i)_{i\in\mathcal{N}}$. Here, we distinguish between $z \in \mathbb{R}^l$ and $y \in \mathbb{R}^n$ with $l \leq n$, where z are temperature measurements and y are internal subsystem energies.

In operation, we always want to consider closed thermal networks, however, from a computational perspective, there are two reasons why open thermal networks may be advantageous. These are: *a)* to reduce model complexity. For example, we can disregard dynamics within the return network, since heat exchanger return temperatures are typically intentionally maintained at a constant level. Consequently, their inclusion in the model is not strictly necessary or even beneficial [6], and *b)* to reduce unwanted effects of discretization. For instance, for implicit discretization schemes (simulation section), there is an implicit dependency on the previous state that propagates backwards. In closed systems, this means that the effect of the discretization propagates back until it reaches the starting point. This results in rather extreme averaging effects for large mass flows, in particular, for systems with few states.

III. STRICT DISSIPATIVITY OF THERMAL NETWORKS

In this section, we establish strict dissipativity, both analytically and numerically, for open and closed thermal networks introduced in the previous section. We require this property to ensure certain guarantees for the EMPC algorithm for DHS given in the next section.

Definition 3 (Strict dissipativity): A discrete-time dynamical system

$$x(k+1) = f(x(k), u(k)), \quad x(0) = x_0, \tag{11}$$

with $x(k) \in \mathbb{R}^n$, $u(k) \in \mathbb{R}^m$, $f : \mathbb{R}^n \times \mathbb{R}^m \to \mathbb{R}^n$, and $(x(k), u(k)) \in \mathbb{X} \times \mathbb{U}$ is strictly dissipative w.r.t. the supply rate $s(x, u) = \ell(x, u) - \ell(x^*, u^*)$ and the optimal steady state $(x^*, u^*) \in \mathbb{X}\times\mathbb{U}$, if there exists a storage function $\lambda : \mathbb{X} \to \mathbb{R}$ bounded from below on $\mathbb{X}$ and a function $\zeta \in \mathcal{K}_\infty$ such that for all $(x, u) \in \mathbb{X} \times \mathbb{U}$,

$$\lambda(f(x, u)) - \lambda(x) \leq s(x, u) - \zeta(|x - x^*|). \tag{12}$$

A. Dissipativity of closed thermal networks

We apply an explicit Euler discretization to system (2) to obtain:

$$Vx(k+1) = Vx(k) + A_c(q)x(k) + B_p h_p(k) - B_d h_d, \tag{13}$$

where we decomposed $Bh(k)$ into a controllable part $B_p h_p(k)$ and a known (constant) disturbance $-B_d h_d$, where $h_p \in \mathbb{R}^{n_p}$ and $h_d \in \mathbb{R}^{n_d}$ represent the producer nodes and demand nodes, respectively, and $B_p \in R^{n\times n_p}$ and $B_d \in \mathbb{R}^{n\times n_d}$ consist of augmented column vectors that have exactly one element equal to 1 at the node that is active.

Theorem 1: The discrete-time *closed* thermal network (13) is strictly dissipative with respect to the supply rate $\hat{\ell}(x, h_p, q) = \ell(x, h_p, q) - \ell(x^*, h_p^*, q^*)$ and the optimal steady state $(x^*, h_p^*, q^*) \in \mathbb{Z} = \mathbb{X} \times \mathbb{U} \times \mathbb{Q}$ with a linear storage function $\lambda(x) = \gamma \mathbf{1}^\top V x$ and a linear cost function $\ell(x, h_p, q) = r^\top h_p$, where $r = \gamma \mathbf{1}^\top B_p$ as long as $\gamma \neq 0$.

Proof: We apply Definition 3 to system (13) to obtain

$$\begin{aligned} \lambda\left(V^{-1}(A_c(q)x + B_p h_p - B_d h_d)\right) \\ \leq r^\top h_p - r^\top h_p^* - \zeta(|x - x^*|), \end{aligned}$$

which then can be separated into two inequalities, where we apply $\lambda(x) = \gamma \mathbf{1}^\top V x$:

$$\begin{aligned} \gamma \mathbf{1}^\top A_c(q)(x - x^*) &\leq -\zeta(|x - x^*|), \\ \gamma \mathbf{1}^\top A_c(q)x^* + \gamma \mathbf{1}^\top (B_p h_p - B_d h_d) &\leq r^\top (h_p - h_p^*). \end{aligned}$$

Due to mass conservation, we have that multiplying from the left with $\mathbf{1}^\top$ cancels out all dependency on q such that $\mathbf{1}^\top A_c(q) = -\mathbf{1}^\top D_\alpha$. Furthermore, it is easy to check that any equilibrium $(x_e, h_{p,e}, q_e) \in \mathbb{Z}$, not necessarily optimal, has to satisfy $\sum_{i=1}^{n_p} h_{p,e,i} = \sum_{i=1}^{n_d} h_{d,i} + \sum_{i=1}^{n} \alpha_i x_{e,i}$ (energy balance). With this, we are able to state the following two conditions required for strict dissipativity:

$$-\gamma \sum_{i=1}^{n} \alpha_i (x_i - x_i^*) \leq -\zeta(|x - x^*|), \tag{14}$$

and

$$\begin{aligned} \underbrace{-\gamma \sum_{i=1}^{n} \alpha_i x^* + \gamma \left(\sum_{i=1}^{n_p} h_{p,i}^* - \sum_{i=1}^{n_d} h_{d,i} \right)}_{=0} \\ + \gamma \sum_{i=1}^{n_p} (h_{p,i} - h_{p,i}^*) \leq r^\top (h_p - h_p^*), \end{aligned} \tag{15}$$

which is satisfied for $r^\top = \gamma \mathbf{1}^\top B_p$. Then, the optimal equilibrium temperature must be minimal if $\gamma > 0$, and maximal if $\gamma < 0$ for (14) to hold for any $x \in \mathbb{X}$.[1] To illustrate, in Fig 4, we compare the two planes for any (arbitrary) equilibrium point $x_{eq} \in \mathbb{X}$. When $x_{eq} > x_{\min}$, we find that the dissipation inequality is not satisfied for part of the feasible set, and we do not have strict dissipativity. Hence, we require $x_{eq} = x_{\min} = x^*$ for strict dissipativity. ■

B. Dissipativity of open thermal networks

Again, here we apply an explicit Euler discretization to (10) to obtain:

$$Vx(k+1) = Vx(k) + A_o(q)x(k) + B_o u_o(k) - B_d h_d, \tag{16}$$

but we assume $h_p = 0$, since we can control heat insertion through $u_o(k) \in \mathbb{R}^{n_o}$.

[1] For $\gamma = 0$ we have only dissipativity, not strict dissipativity.

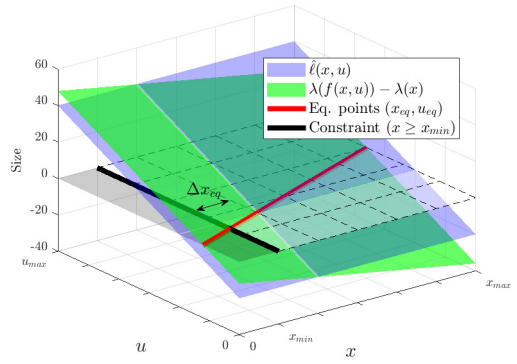

Fig. 4. Illustrating hyperplanes of the (difference in) storage function and supply rate. Strict dissipativity holds when the blue plane is above the green plane within the feasible set. Note that the slope of the red line, which encodes the effect of heat losses, has been greatly exaggerated for illustrative purposes. The distance measure $\Delta x_{eq} > 0$ suggests a subset of the feasible set does not satisfy the dissipation inequality.

Theorem 2: The discrete-time *open* thermal network (16) is strictly dissipative with respect to the supply rate $\hat{\ell}(x, u_o, q) = \ell(x, u_o, q) - \ell(x^*, u_o^*, q^*)$ and the optimal steady state $(x^*, u_o^*, q^*) \in \mathbb{Z} = \mathbb{X} \times \mathbb{U} \times \mathbb{Q}$ with a linear storage function $\lambda(x) = \gamma \mathbf{1}^\top V x$ and a linear cost function $\ell(x, u_o, q) = \gamma \mathbf{1}^\top (B_o u_o - B_d B_d^\top Q x)$.

Proof: The result is similar to the proof for closed thermal networks (Theorem 1). The main difference is that in this case, we get an additional term from $\mathbf{1}^\top A_o(q)x = -\sum_{i=1}^n \alpha_i x_i - \mathbf{1}^\top B_d B_d^\top Q x$. Nonetheless, just like in the closed thermal network case, we can write the first inequality centered around x^* to obtain

$$-\gamma \sum_{i=1}^{n} \alpha_i (x_i - x_i^*) \leq -\zeta(|x - x^*|).$$

Then, the remaining parts are used to form the second inequality

$$\underbrace{-\gamma \left(\sum_{i=1}^{n} \alpha_i x_i^* + \mathbf{1}^\top B_d B_d^\top Q^* x^* + \mathbf{1}^\top B_d h_d - \mathbf{1}^\top B_o u_o^* \right)}_{=0}$$
$$+ \gamma \mathbf{1}^\top \left(B_o (u_o - u_o^*) - B_d B_d^\top (Qx - Q^* x^*) \right) \leq \hat{\ell}(x, u_o, q),$$

which we simplify by defining $\Delta u := \mathbf{1}^\top (B_o u_o - B_d B_d^\top Q x)$. This change results in the following inequality:

$$\gamma(\Delta u - \Delta u^*) \leq \hat{\ell}(x, u_o, q),$$

and, consequently, we have to satisfy this with equality if $\Delta u_{\min} < \Delta u^* < \Delta u_{\max}$. Therefore, in analogy with the closed example, we have strict dissipativity with respect to the state whenever x^* is minimal (for $\gamma > 0$) and maximal (for $\gamma < 0$). ∎

Remark 2: This particular cost function represents the difference between the sum of energy at each pipe inlet and the sum of energy of the flow exiting the pipe after each consumer.

Remark 3: Both results for closed and open thermal networks rely on using a specific cost function that is linear in the input energy. Moreover, we see that this assumption yields strict dissipativity for a specific equilibrium on the boundary of our constraint set, and with respect to x only. This begs the question whether other cost functions, or strictness with respect to the input, are a possibility. Analytically, it is difficult to construct higher order storage functions to allow for various meaningful cost functions, but numerically, we can increase the complexity of the storage functions. Motivated by this, we present a numerical approach in the following section.

C. Numerical verification of strict dissipativity

In this section, we provide a numerical approach to verifying strict dissipativity. We extend the definition to strictness with respect to both state and input, therefore, we introduce the notation $|(a, b)|_{a^*, b^*} = ||a - a^*|| + ||b - b^*||$.

1) Method: Contrary to an analytical approach, in a numerical approach, we have the ability to expand the range of potential storage functions, which enhances our prospects of identifying a storage function that satisfies strict dissipativity for any specified cost function. On the other hand, we are restricted to evaluate systems of low dimension due to high computational demands.

In short, the objective is to find a function $\lambda : \mathbb{R}^n \to \mathbb{R}$ from a given set $\Lambda = \{\lambda\}$ and a scalar $\sigma \in \mathbb{R}$ that satisfy the following inequality:

$$\ell(x, u) - \sigma + \lambda(x) - \lambda(f(x, u)) - \zeta(|(x, u)|_{x^*, u^*}) \geq 0, \quad (17)$$

for a discrete-time system (11) by writing an optimization problem as follows:

$$\begin{aligned} \max_{\sigma \in \mathbb{R},\ \lambda \in \Lambda} \quad & \sigma, \\ \text{s.t.} \quad & (17), \\ & g_i(x, u) \geq 0, \quad \forall i = \{1, \ldots, l\}, \end{aligned} \quad (18)$$

where $g : \mathbb{R}^{n+m} \to \mathbb{R}^l$ comprises all state and input constraints, i.e., $(x, u) \in \mathbb{X} \times \mathbb{U}$. Problem (18) is a semi-infinite optimization, which is generally hard to solve. Instead, we implement a relaxation based on the S-procedure, as was done in [19]. This procedure makes use of sum of squares (SOS) programming by defining Λ as a set that contains parameterized polynomial basis functions of x up to a certain degree d. Subsequently, rather than proving the inequality in (18) directly, the goal is to prove that there exists a $\lambda \in \Lambda$ such that the left hand side of (17) can be written in SOS formulation [20]. Furthermore, by introducing SOS multiplier variables $\mu_i : \mathbb{R}^{n+m} \to \mathbb{R}$ for each constraint $g_i(x, u),\ i = \{1, \ldots, l\}$, which are polynomial basis functions themselves, we can rewrite all inequalities $g_i(x, u) \geq 0$ within the dissipativity inequality.

As a result, we get the following polynomial optimization

problem:

$$\begin{aligned} \max_{\sigma\in\mathbb{R},\ \lambda\in\Lambda} \quad & \sigma, \\ \text{s.t.} \quad & \ell(x,u) - \sigma + \lambda(x) - \lambda(f(x,u)) \\ & - \zeta(|(x,u)|_{x^*,u^*}) - g(x,u)^\top \mu \geq 0, \end{aligned} \tag{19}$$

which can be solved efficiently using sum of squares. The solution σ^* represents a lower bound on the optimal stage cost $\ell(x^*,u^*)$; see [20]. Simultaneously, we require $\sigma^* \geq \ell(x^*,u^*)$ to satisfy the inequality in (17). Thus, concluding that we need $\sigma^* = \ell(x^*,u^*)$.

2) Results: We tested a set of cost functions for the following open thermal network with two states:

$$\begin{bmatrix} x_1 \\ x_2 \end{bmatrix}^+ = \begin{bmatrix} 1-\frac{q+\alpha}{V} & 0 \\ \frac{q}{V} & 1-\frac{q+\alpha}{V} \end{bmatrix} \begin{bmatrix} x_1 \\ x_2 \end{bmatrix} + \begin{bmatrix} \frac{q}{V} \\ 0 \end{bmatrix} x_o + \begin{bmatrix} 0 \\ \frac{1}{V} \end{bmatrix} h_d, \tag{20}$$

where we substituted $u_o(k) = q(k)x_o(k)$ in (16), where $q(k)$ is the mass flow and $x_o(k)$ is the pipe inlet temperature. Also, h_d is the extracted heat. The system is subject to box constraints $g(x,x_o,q) \leq 0$.

We choose a set of storage functions $\Lambda = \{\theta \in \mathbb{R}^6 | \lambda(x) = \sum_{d=1}^{3} \theta_d x_1^d + \theta_{d+3} x_2^d\}$ and, similarly, define a set of multiplier functions of degree 1. Then, we solve problem (19) to find σ^*. To confirm if σ^* guarantees strict dissipativity, we solve a separate optimization problem to find the value of the cost at the optimal equilibrium, i.e., $\ell(x^*,x_o^*,q^*) = \min\{\ell(x,x_o,q) |$ s.t. $x = f(x,x_o,q),$ and $(x,x_o,q) \in \mathbb{Z}\}$.

Thus, we are able to confirm strict dissipativity with respect to state and input, whenever $\sigma^* \geq \ell(x^*,x_o^*,q^*)$. Table I contains four possible cost functions with different equilibrium points for which this is the case.

TABLE I

EXAMPLES OF COST FUNCTIONS THAT GUARANTEE STRICT DISSIPATIVITY

Stage cost	Equilibrium
$\ell = Rx_o^2 + q^2,\ R \geq 1/\rho^2$	Minimum inputs
$\ell = (x_o - x_{o,R})^2 + (q - q_R)^2$	Reference setpoints $(x_{o,R}, q_R)$
$\ell = -qx_1$	Maximum supply temp. and flow
$\ell = (qx_1 - E_R)^2$	Satisfies reference $q^*x_1^* = E_R$

Remark 4: We used $\zeta = \epsilon|(x,x_o,q)|_{x^*,x_o^*,q^*}$ as a $\mathcal{K}_\infty$ function with $\epsilon = 10^{-7}$ to enforce strictness of the inequality with respect to states *and* inputs.

IV. ECONOMIC NONLINEAR MODEL PREDICTIVE CONTROL

In this section, we summarize a set of results from the literature on EMPC. In particular, we refer the reader to works such as [13], [14], [15], [16], for details on the methods and proofs. Here, we only state the important concepts relevant for this work, which are mostly related to the time-varying case, as presented in [14].

A. Problem formulation

Consider the *time-varying* discrete-time dynamics

$$x(k+1) = f_k(x(k),u(k)), \quad x(0) = x_0, \tag{21}$$

with $x(k) \in \mathbb{R}^n$, $u(k) \in \mathbb{R}^m$, $k \in \mathbb{N}$, and $f_k : \mathbb{R}^n \times \mathbb{R}^m \to \mathbb{R}^n$.

The receding horizon optimal control problem without terminal conditions is defined as

$$\begin{aligned} V_{N,k}(x_k) = \min_{x_N,u_N} \quad & \sum_{i=k}^{k+N-1} \ell_i(x(i),u(i)), \\ \text{s.t.} \quad & x(i+1) = f_i(x(i),u(i)), \\ & x(i) \in \mathbb{X}_i, \quad u(i) \in \mathbb{U}_i, \\ & i = \{k,\dots,k+N-1\}, \\ & x(k) = x_k. \end{aligned} \tag{22}$$

The solution of the optimal control problem is an optimal trajectory (x_N^*, u_N^*) for a specified horizon $N \in \mathcal{T}$. In MPC, the optimal control problem in (22) is solved iteratively. In each step, the feedback control law

$$\mu_{N,k}(x_k) = u_N^*(0)$$

is applied to the system. Generally, to ensure stability of the closed-loop system, a terminal cost and constraint are required. These conditions will ensure that the closed-loop converges to the infinite-horizon optimal trajectory. However, for nonlinear time-varying systems, it is not straightforward to compute these terminal ingredients, and in EMPC we typically do not have any knowledge of optimal trajectories. Instead, we are interested in showing whether the solution of the closed-loop MPC without terminal conditions approximates the solution of the infinite horizon problem. To this end, we introduce the following definitions.

Definition 4 (Time-varying strict dissipativity [14]): A discrete-time system (21) is strictly dissipative with respect to the supply rate $s_k(x,u) = \ell_k(x,u) - \ell_k(x^*(k),u^*(k))$ and the optimal trajectory $(x^*(k),u^*(k)) \in \mathbb{X}_k \times \mathbb{U}_k$ if there exists a storage function $\lambda_k : \mathbb{N} \times \mathbb{X}_k \to \mathbb{R}$ bounded from below on $\mathbb{X}_k$ with $\zeta \in \mathcal{K}_\infty$ such that for all $(x,u) \in \mathbb{X}_k \times \mathbb{U}_k$ and for all $k \in \mathbb{N}$, we have

$$\begin{aligned} & \ell_k(x,u) - \ell_k(x^*(k),u^*(k)) \\ & + \lambda_k(x) - \lambda_k(f_k(x,u)) \geq \zeta(|(x,u)|_{x^*(k),u^*(k)}). \end{aligned} \tag{23}$$

Assumption 5 (Continuity of $V_{N,k}$ at x^* [14]): There exists a function β_V such that for each $x \in \mathbb{X}, k \in \mathbb{N}, N \in \mathcal{T}$, the following holds:

$$|V_{N,k}(x) - V_{N,k}(x^*(k))| \leq \beta_V(|x|_{x^*(k)}). \tag{24}$$

This assumption also means that the optimal value function is bounded.

Strict dissipativity and boundedness of the optimal value functions are sufficient conditions for the existence of the turnpike property in time-varying systems [17]. Intuitively, the turnpike property suggests that the closed-loop EMPC solution remains close to the optimal trajectory for the majority of the time. As it turns out, the turnpike property will guarantee us three key properties regarding the performance of the EMPC [15]. These are: approximate optimality, convergence to the optimal trajectory, and recursive feasibility.

B. Application to thermal systems

We have already shown that the time-invariant system (13) is strictly dissipative for $\ell(x, h_p, q) = r^\top h_p$ when a constant disturbance h_d is acting on the system. That said, the strict dissipativity property extends directly to the time-varying case as in (23) with $h_d = h_d(k)$. This follows from the fact that, in each time instance k, we can perform the same analysis for the corresponding optimal equilibrium, i.e., the equilibrium for which $\sum_{i=1}^{n_p} h^*_{p,i}(k) = \sum_{i=1}^{n_d} h_{d,i}(k) + \sum_{i=1}^{n} \alpha_i x^*_i(k)$, to satisfy the dissipation inequality. In the open case of (20), we have also proven that we can have strict dissipativity with different cost functions at different equilibrium points. Even though we were only able to verify this on a small-scale system, we believe that the addition of thermal nodes in an open network should not affect the result.

V. SIMULATIONS

In this section, we consider a three consumer, one producer district heating network. The network is modeled as a tree structure, where all the flow from the producer is distributed to the consumers through a supply pipe. Each consumer has its own time-varying demand $h_{d,i} > 0$. The layout is illustrated in Fig 5.

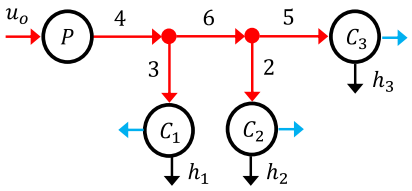

Fig. 5. DHS layout for simulations. The numbers on the edges denote the pipe length in kilometers.

We assume the return pipe has a constant temperature, and therefore, we do not include it in the model. Thus, the model of the network is derived from the open thermal network (10). A spatial discretization step of 500 meter is used, and, as a result, we have $n = 40$ states in the model.

A. Discretization

In order to solve the optimal control problem we require a discrete-time model of the system. Thermal systems typically have large inertia, and their dynamics change relatively slowly. Moreover, it is desirable to have sufficient time for solving the optimal control problems to ensure tractability. Therefore, it is preferable to work with large time steps (i.e., 15 minutes to 1 hour); see [7] for more details.

For explicit discretization schemes, a necessary condition for convergence of the numerical solution of a partial differential equation (PDE) is called the Courant-Friedrichs-Lewy (CFL) condition, which states that the displaced mass in one time step is less than or equal to the volume of each cell, i.e., $q(k)\tau \leq V,\ k \in \mathbb{N}$.

In general, it might be difficult to satisfy this condition, especially if we want to (accurately) model pipes using finite volume cells (i.e., thermal nodes). Hence, an implicit discretization is preferred, since it always results in a numerically stable discretization. This discretization is defined by

$$x(k+1) = x(k) + \tau f(x(k+1), u(k+1)), \tag{25}$$

which means that the implicit discretization of (10) is

$$\begin{aligned} x(k+1) = {} & F_o(q(k))x(k) \\ & + G_o(q(k))x_o(k) - G_d(q(k))h_d(k), \end{aligned} \tag{26}$$

where $F_o(q(k)) = \left(I - \tau V^{-1} A_o(q(k))\right)^{-1}$, $G_o(q(k)) = \tau F_o(q(k)) V^{-1} B_o q_o(k)$, and $G_d(q(k)) = \tau F_o(q(k)) V^{-1} B_d$. Moreover, we have substituted $u_o(k) = q_o(k) x_o(k)$ and shifted the index in $q(k+1)$, $x_o(k+1)$, and $h_d(k+1)$ backwards by one because they are piecewise constant functions. Therefore, they are constant between any time step k and $k+1$, and the shift will not affect the model.

B. Settings

The cost function is chosen as a weighted norm of the temperature at the inlet and the mass flow at the inlet, i.e., $\ell(x_o, q_o) = 50 p_k x_o^2 + \rho^2 q_o^2$, with time-varying parameter $p_k = 0.5$ if $k \in [10, 15]$ and $p_k = 1$ otherwise. This cost function encourages minimization of temperature in the network, while also penalizing the flow rate, but also allows flexibility to build up a buffer during off peak hours. To give the controller sufficient time to react to demand and/or price variations, we choose a prediction horizon of $N = 8$ and time step $\tau = 3600$. Furthermore, constraints have been added to restrict large changes in inputs between time steps, which avoids fast switching. We solve the nonlinear EMPC problem (22) using IPOPT. Subsequently, we apply the first element of the optimal sequence of inputs computed in the optimization to the same system at a much finer discretization with ten times as many states simulated with a time step of one second using an ODE solver.

The results of Fig 6 show that the controller is able to maintain sufficient supply temperature for each of the consumers. At the same time, there is a period during the middle of the day where the heat production is ramped up to account for the evening peak. In addition, we find that

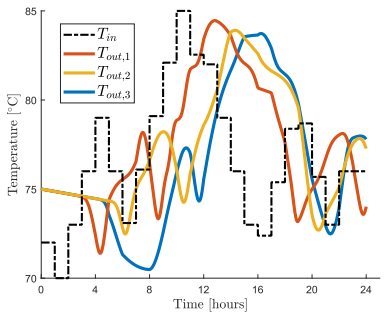

Fig. 6. The pipe inlet temperature and the observed outlet temperatures at the consumers with $T_{in} = x_o$ and $T_{out,i} = x_{n_{c,i}}$.

in our simulations the open-loop trajectories generated by the EMPC stay near the closed-loop optimal trajectory, but

diverge towards the end, as can be seen in Fig 7. This observation further supports our conjecture that the system exhibits the turnpike property.

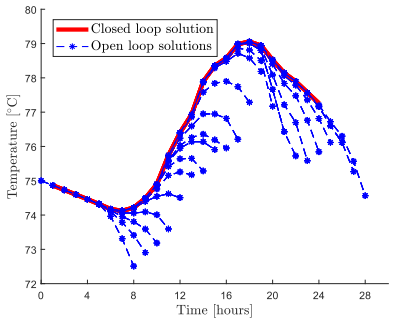

Fig. 7. The predicted outlet temperature at consumer 3: the closed loop solution versus the open loop solutions at each iterate.

VI. DISCUSSION AND CONCLUSION

We presented two different models that can be used in the context of MPC for DHS, derived from partial differential equations governing the heat transport dynamics. We then provided both theoretical guarantees and numerical evidence for the existence of strict dissipativity in these networks, accompanied by a set of practically motivated objective functions that enable approximately optimal economic operation of the controller.

The results from this work have meaningful implications for DHS. In practice, implementing MPC for DHS should remain simple, while also providing users with the ability to customize controller parameters to suit their preferences. Therefore, it is relevant to look at the case of EMPC without terminal conditions. We have provided evidence, and in some cases, demonstrated theoretical validity that the closed-loop solutions of the EMPC are approximately optimal and practically converge towards the optimal trajectory. Hence, these findings can assist practitioners when determining how to design or tune, for example, their objective function through a systematic verification approach. Nonetheless, we should acknowledge that the bridge to actual implementation has not been crossed yet. The verification results have potentially broader applicability to more general models and architectures. Furthermore, our modeling framework and verification approach may prove to be inadequate for certain DHS, e.g., when there are discrete decisions involved. Despite these challenges, the results indicate an important first step towards the integration of EMPC theory for DHS applications.

For future work, the results can be extended to incorporate even more generalized sets of objective functions and model architectures. To this end, we aim to address the challenge of scalability and extend the application of our theory to larger, more complex real-world systems. Additionally, considering the emergence of smart energy systems, we expect that the analysis of a multi-producer network with enhanced emphasis on flexibility, such as through more detailed models for buffers or heat exchangers, would be of substantial value.

ACKNOWLEDGMENT

This work has been funded by the Local Inclusive Future Energy (LIFE) City Project (MOOI32019), funded by the Ministry of Economic Affairs and Climate and by the Ministry of the Interior and Kingdom Relations of the Netherlands.

REFERENCES

[1] S. Paardekoper et al., Heat roadmap Europe 4: quantifying the impact of low-carbon heating and cooling roadmaps. Aalborg Universitetsforlag, 2018.
[2] G. Sandou et al., Predictive control of a complex district heating network. In IEEE Conference on Decision and Control, 44(8), December, 2005, pp. 7372-7377.
[3] F. Verrilli et al., Model predictive control-based optimal operations of district heating system with thermal energy storage and flexible loads. IEEE Transactions on Automation Science and Engineering, 14(2), 2016, pp. 547-557.
[4] F. Agner, P. Kergus, R. Pates, and A. Rantzer, Combating district heating bottlenecks using load control. Smart Energy, 6, 2022.
[5] L. Mitridati, and J.A. Taylor, Power systems flexibility from district heating networks. In 2018 Power Systems Computation Conference (PSCC), IEEE, 2018, pp. 1-7.
[6] M. Rein, J. Mohring, T. Damm, and A. Klar, Optimal control of district heating networks using a reduced order model. Optimal Control Applications and Methods, 41(4), 2020, pp. 1352-1370.
[7] R. Krug, V. Mehrmann, and M. Schmidt, Nonlinear optimization of district heating networks. Optimization and Engineering, 22, 2021, pp. 783-819.
[8] H. Dänschel, V. Mehrmann, M. Roland, and M. Schmidt, Adaptive nonlinear optimization of district heating networks based on model and discretization catalogs. SeMA Journal, 2023. pp. 1-32.
[9] J. Jansen, F. Jorissen, L. Helsen, Optimal control of a fourth generation district heating network using an integrated non-linear model predictive controller. Applied Thermal Engineering, 223, 2023.
[10] V. Adetola and M. Guay, Integration of real-time optimization and model predictive control. Journal of Process Control, 20(2), 2010, pp. 125-133.
[11] A. Gopalakrishnan and L.T. Biegler, Economic nonlinear model predictive control for periodic optimal operation of gas pipeline networks. Computers & Chemical Engineering, 52, 2013, pp. 90-99.
[12] S. Engell, Feedback control for optimal process operation. Journal of Process Control, 17(3), 2007, pp. 203-219.
[13] L. Grüne and J. Pannek, Nonlinear model predictive control. Springer International Publishing, 2017.
[14] L. Grüne and S. Pirkelmann, Economic model predictive control for time-varying system: Performance and stability results. Optimal Control Applications and Methods, 41(1), 2020, pp. 42-64.
[15] L. Grüne, Why does strict dissipativity help in model predictive control? urn:nbn:de:bvb:703-epub-4593-9, Department of Mathematics, University of Bayreuth, Bayreuth, 2020.
[16] T. Faulwasser, L. Grüne, and M.A. Müller, Economic nonlinear model predictive control. Foundations and Trends® in Systems and Control, 5(1), 2018, pp. 1-98.
[17] L. Grüne, S. Pirkelmann, and M. Stieler, Strict dissipativity implies turnpike behavior for time-varying discrete time optimal control problems. Springer International Publishing, 2018, pp. 195-218.
[18] T. Faulwasser, M. Korda, C.N. Jones, amd D. Bonvin, Turnpike and dissipativity properties in dynamic real-time optimization and economic MPC. In 53rd IEEE Conference on Decision and Control, IEEE, December, 2014, pp. 2734-2739.
[19] J. Berberich, J. Köhler, F. Allgöwer, M.A. Müller, Dissipativity properties in constrained optimal control: A computational approach. Automatica, 114, 2020.
[20] S. Pirkelmann, D. Angeli, and L. Grüne, Approximate computation of storage functions for discrete-time systems using sum-of-squares techniques. IFAC-PapersOnLine, 52(16), 2019, pp. 508-513.
[21] J.E. Machado, J. Ferguson, M. Cucuzzella, J.M. Scherpen, Decentralized temperature and storage volume control in multiproducer district heating. IEEE Control Systems Letters, 7, 2022, pp. 413-418.
[22] M. Arcak, C. Meissen, and A. Packard, Networks of dissipative systems: compositional certification of stability, performance, and safety. Springer, 2016.